Supporting Information for

A cationic iridium(III) complex with aggregation-induced emission (AIE) property for highly selective detection of explosives

Xue-Gang Hou, Yong Wu, Hong-Tao Cao, Hai-Zhu Sun, Hai-Bin Li, Guo-Gang Shan* and Zhong-Min Su*

Institute of Functional Material Chemistry, Faculty of Chemistry, Northeast Normal University, Changchun 130024, People's Repubic of China; Fax: +86-431-85684009 Tel.: +86-431-85099108, E-mail: shangg187@nenu.edu.cn, zmsu@nenu.edu.cn

1. Theoretical calculations

Calculation on the ground and excited electronic state of complexes were investigated by preforming DFT and TD-DFT at B3LYP level. The 6-31G* basis sets were employed for optimizing the C, H, N atoms and the LANL2DZ basis sets for Ir atom. An effective core potential (ECP) replaces the inner core electrons of iridium leaving the outer core $(5s)^2(5p)^6$ electrons and the $(5d)^6$ valence electrons of Ir(III). The geometry of the metal-centered triplet (^{3}MC) was fully optimized and was calculated at the spin-unrestricted UB3LYP level with a spin multiplicity of 3. All expected values calculated for S^2 were smaller than 2.05.All calculations reported here were carried out with the Gaussian 09 software package.[1]

Table S1 The calculated energy levels of the lower-lying transitions of complex **1**.

Complex	States	Assignment	eV	*f*	Nature
1	T_1	H→L (100%)	2.47	0	^{3}ILCT
	T_2	H-1→L (87%)	2.63	0	^{3}MLCT/^{3}LLCT
	T_3	H-1→L+1(49%)	2.75	0	^{3}MLCT/^{3}LLCT

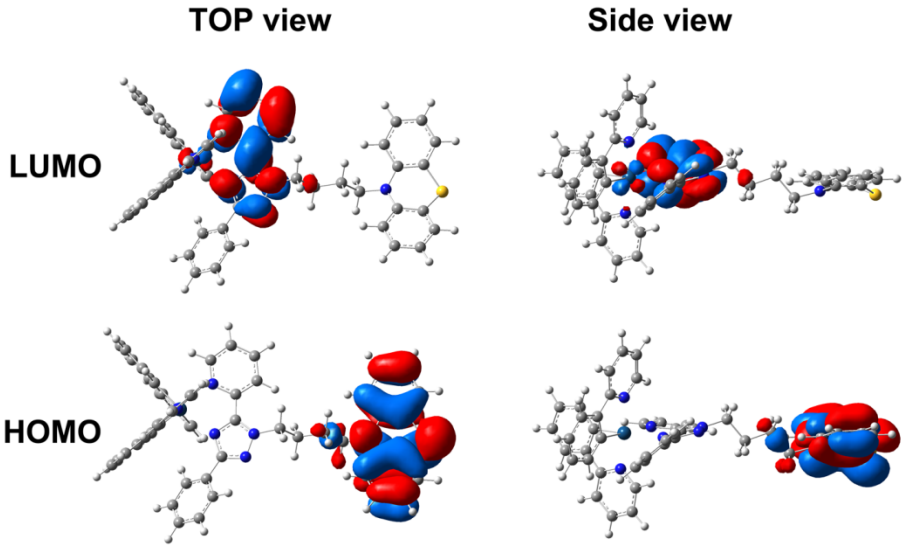

Fig. S1. Molecular orbitals involved in the excitation of complex **1**.

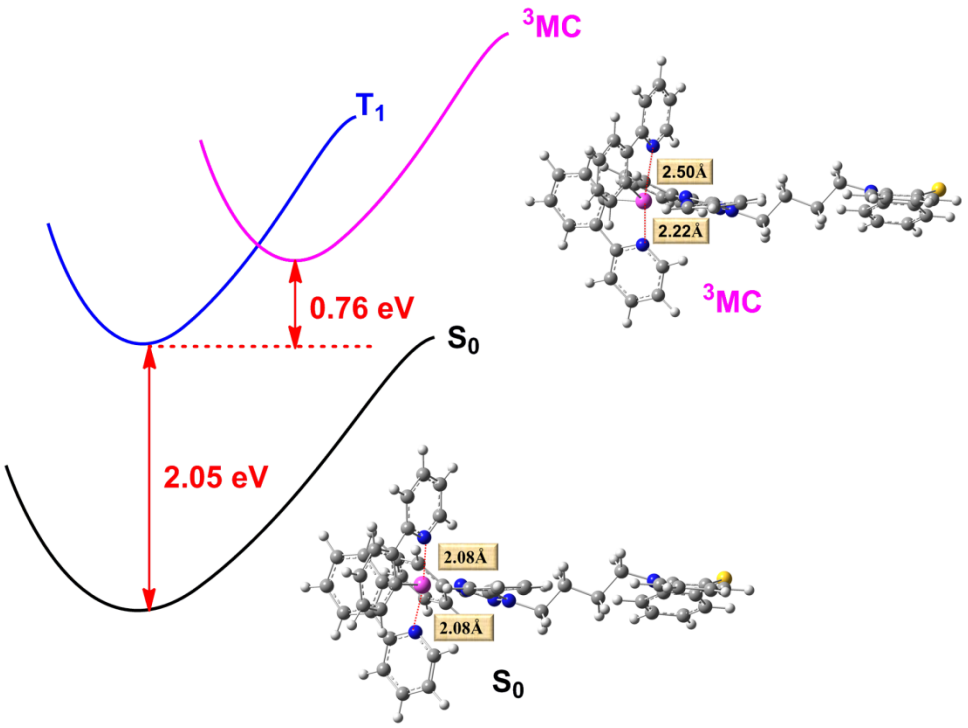

Fig. S2. Schematic energy diagram showing the adiabatic energy differences calculated between the S_0, T_1 and ^{3}MC states and the computed Ir-$N_{cyclometalated\ ligand}$ bond lengths in corresponding S_0 and ^{3}MC states.

2. Experimental general information

All reagents and solvents employed were commercially available and used as received without further purification. The solvents for syntheses were freshly distilled over appropriate drying reagents. All experiments were performed under a nitrogen atmosphere by using standard Schlenk techniques. ^{1}H NMR spectra were measured on Bruker Avance 500 MHz with tetramethylsilane as the internal standard. The molecular weights of ligands and complexes were tested by using electrospray-ionization mass spectroscopy and matrix-assisted laser desorption-ionization time-of-flight (MALDI-TOF) mass spectrometry, respectively. IR spectrum was performed in the range 4000 – 400 cm^{-1} using KBr pellets on an Alpha Centaurt FT/IR spectrophotometer. UV-vis absorption spectra were recorded on Hitachi U3030 spectrometer. The emission spectra were recorded using the F-4500 FL spectrophotometer. The excited-state lifetime were measured on a transient spectrofluorimeter (Edinburgh FLS920) with time-correlated single-photon counting

technique. The photoluminescence quantum yields (PLQYs) of the neat film were measured in an integrating sphere. Transmission electron microscopy (TEM) and electron diffraction pattern of sample were performed using a TECNAI F20 microscope. The samples were prepared by placing microdrops of colloid solution on a holey carbon copper grid.

3. Synthesis and characterization of ancillary ligand (L) and complex 1

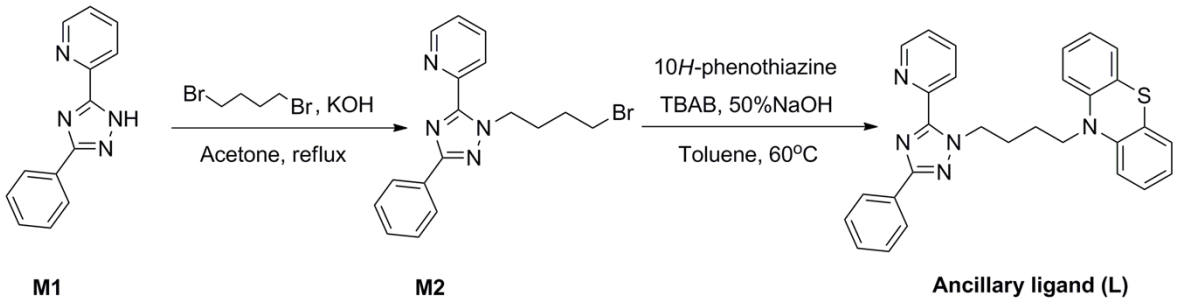

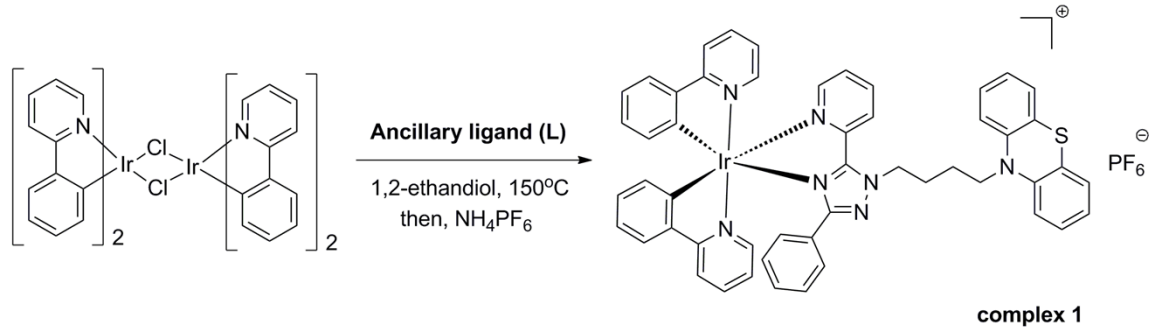

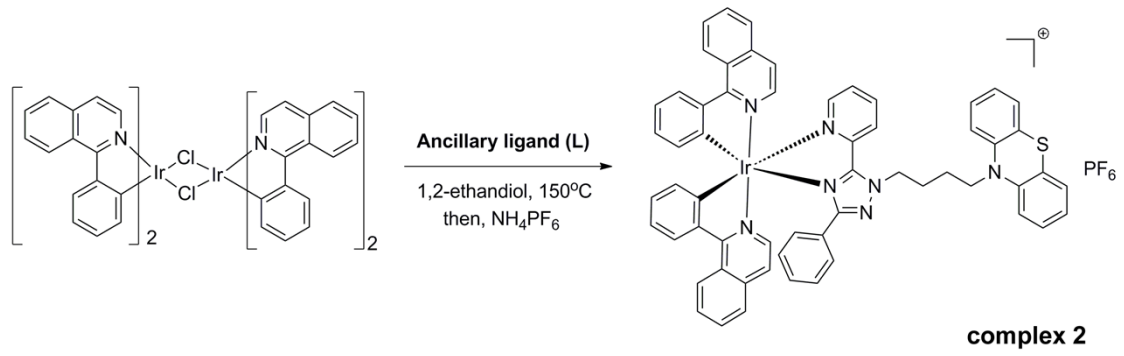

Scheme S1 Synthetic routes of ancillary ligand **L** and complex **1** and the reference complex **2**.

3.1 Synthesis of 2-(1-(4-bromobutyl)-3-phenyl-1H-1,2,4-triazol-5-yl)pyridine (M2)

A mixture of the precursor 2-(3-phenyl-1*H*-1,2,4-triazol-5-yl)pyridine (M1) (1.1 g, 5.0 mmol) prepared according to previous report[2] was dissolved in acetone (30 mL), and the equivalent KOH was added and the mixture was stirred for 0.5 h. Then, 1,4-dibromobutane (1.18g, 5.5mmol) in 5 mL acetone was added into the reaction system and the mixture was heated to reflux for overnight. After cooling to room temperature, the mixture was quenched by water and then extracted by dichloromethane. The organic layer was dried with Na_2SO_4 and the solvent was removed. The obtained residues was purified by column chromatography on silica gel with ethyl acetate/petroleum ether (1:3) as the eluent to yield the white solid (51%). ^{1}H NMR (500 MHz, $CDCl_3$, ppm): δ 8.68–8.69 (m, 1H), 8.34 (d, J = 8 Hz, 1H), 8.16–8.18 (m, 2H), 7.84–7.86 (m, 1H), 7.35–7.48 (m, 4H), 4.92 (t, J = 7.0 Hz, 2H), 3.48 (t, J = 6.5 Hz, 2H), 2.17 (t, J = 7.5 Hz, 2H), 1.94–1.97 (m, 2H). ^{13}C NMR (126 MHZ, $CDCl_3$, ppm): 160.7, 152.2, 148.8, 147.9, 136.9, 130.9, 129.1, 128.5, 126.3, 124.0, 123.9, 49.8, 33.0, 29.5, 28.7. IR (cm^{-1}): v = 3429 (w), 3053 (w), 2953 (m), 1953 (w), 1584 (m), 1521 (w), 1470 (s), 1348 (m), 1251 (m), 1150 (w), 1064 (m), 1029 (s), 896 (w), 797 (s), 725(s), 688 (s), 558 (m), 489 (m). MS (MALDI-TOF): m/z 357.1 (M+H).

3.2 Synthesis of ancillary ligand (L)

A mixture of M2 (1.20g 3.36mmol), 10H-phenothiazine (0.90g, 4.5mmol), 50%NaOH (10mL) and tetrabutyl ammonium bromide (TBAB, 0.8g) in 20 mL toluene was heated at 60^{o}C for 6 h under argon. After cooling to room temperature, the mixture was extracted with CH_2Cl_2. After washing with water, drying over anhydrous Na_2SO_4, and evaporating the solvents, we purified the residue by column chromatography on silica gel using the ethyl acetate/petroleum ether (1:6) as eluent, yielding the white solid (**L**). Yield: 47%. ^{1}H NMR (500 MHz, $CDCl_3$, ppm): δ 8.50–8.51 (m, 1H), 8.28 (d, J = 8 Hz, 1H), 8.15–8.16 (m, 2H), 7.79–7.83 (m, 1H), 7.38–7.47 (m, 3H), 7.25–7.30 (m, 1H), 7.06–7.11 (m, 4H), 6.80–6.90 (m, 4H), 4.88 (t, J = 7.0 Hz, 2H), 3.91 (t, J = 7.0 Hz, 2H), 2.04–2.14 (m, 2H), 1.86–1.92 (m, 2H). ^{13}C NMR (126 MHZ, $CDCl_3$, ppm): 160.6, 152.2, 148.8, 147.9, 145.1, 136.9, 131.0,

129.0, 128.5, 127.4, 126.3, 125.2, 123.9, 122.4, 114.4, 50.4, 46.6, 27.5, 23.6. IR (cm^{-1}): ν = 3445 (w), 3053 (w), 2954 (w), 2869 (w), 1590 (m), 1568 (m), 1458 (s), 1441 (s), 1377 (m), 1284 (m), 1156 (m), 1071 (w), 1037 (m), 927 (w), 795 (m), 750 (s), 727 (s), 693(s), 622 (w). MS (MALDI-TOF): m/z 476.2 (M+H).

3.3 Synthesis of the chloro-bridged dimer $[Ir(ppy)_2Cl]_2$

The organometallated dimer $[Ir(ppy)_2Cl]_2$ was synthesized from reaction of $IrCl_3 \cdot 3H_2O$ (0.81 g, 2.32 mmol) with 2-phenylpyridine (ppy, 0.79 g, 5.1 mmol) in 2-ethoxyethanol and water mixture (V:V = 3:1, 40 mL) for 24 h. The mixture was treated with water (30 mL) to induce precipitation of the yellow solid. The product was filtered out and washed with diethyl ether followed by ethanol and dried (yield: 78%).

3.4 Synthesis and characterization of $[Ir(ppy)_2(L)](PF_6)$ (1)

A solution of ligand **L** (1.0 g, 2.1 mmol) and the dichloro-bridged diiridium complex $[Ir(ppy)Cl]_2$ (1.1 g, 1.0 mmol) in 1,2-ethandiol (30 mL) was heated at 150 ^oC for 15 h in the dark. After cooling to room temperature, the aqueous solution of NH_4PF_6 (2.0g in 100 mL of deionized water) was slowly added into the reaction mixture under stirring. The obtained yellow suspension was filtrated, and washed with water and methanol. The crude product was purified by silica gel column chromatography using dichloromethane/ethyl acetate (6:1). The product was then recrystallized from dichloromethane and petroleum ether mixture, yielding a yellow powder (61%). ^1H NMR (500 MHz, d_6–DMSO, ppm): δ 8.55 (d, J = 8.5 Hz, 1H), 8.37 (d, J = 5.0 Hz, 1H), 8.29 (d, J = 8.0 Hz, 1H),8.15–8.18 (m, 1H), 7.94–7.98 (m, 2H), 7.90 (d, J = 6.5 Hz, 1H), 7.76–7.79 (m, 2H), 7.63–7.69 (m, 2H), 7.37 (d, J = 6.5 Hz, 1H), 7.21–7.24 (m, 1H), 7.11–7.16 (m, 5H), 6.81–7.07 (m, 11H), 6.58–6.66 (m, 2H), 6.05 (d, J = 6.5 Hz, 1H), 5.89 (d, J = 6.5 Hz, 1H), 4.91–4.95 (m, 1H), 4.78–4.82 (m, 1H), 3.99 (t, J = 7.0 Hz, 2H), 2.07–2.18 (m, 2H), 1.76–1.78 (m, 2H). ^{13}C NMR (126 MHZ, d_6–DMSO, ppm): 167.5, 166.8, 160.8, 156.7, 150.9, 149.4, 148.7, 148.2, 145.3, 144.7, 144.3, 143.9, 140.3, 139.3, 131.9, 131.3, 130.8, 129.8, 129.7, 129.3, 128.1, 127.9, 127.8, 126.6, 125.7, 124.7, 124.5, 124.3, 123.7, 123.1, 122.9, 121.9, 120.6, 119.9, 116.5,

51.9, 46.3, 26.2, 23.8. IR (cm^{-1}): *v* = 3432 (m), 3061 (w), 2924 (w), 1607 (m), 1479 (m), 1286 (w), 1163 (w), 1032 (w), 841 (s), 791 (w), 754 695 (m), 557 (s). MS (MALDI-TOF): m/z 976.3 (M–PF6). Anal. calcd. For $C_{51}H_{41}F_6IrN_7SP$: C 54.63, H 3.69, N 8.75; found: C 54.92, H 3.96, N 8.85.

3.5 Synthesis and characterization of the reference complex $[Ir(pq)_2(L)](PF_6)$ (2)

The synthesis of complex **2** was similar to that of complex **1** except that the cyclometalated ligand **ppy** was replaced with **pq**. The crude product was also purified by silica gel column chromatography using ethyl acetate to yield complex **2** (58%). ^1H NMR (500 MHz, d_6–DMSO, ppm): δ 9.06 (d, *J* = 7.5 Hz, 1H), 8.55 (d, *J* = 8.5 Hz, 1H), 8.45 (d, *J* = 6 Hz, 1H), 8.41 (d, *J* = 8.5 Hz, 2H), 8.11–8.16 (m, 2H), 7.91–7.96 (m, 2H), 7.76–7.86 (m, 3H), 7.69–7.71 (m, 2H), 7.56–7.65 (m, 3H), 7.23 (d, *J* = 6.5 Hz, 1H), 7.09–7.16 (m, 6H), 6.83–6.91 (m, 9H), 6.72 (t, *J* =8 Hz, 1H), 6.60 (t, *J* =8 Hz, 1H), 6.36 (d, *J* =7.5 Hz, 1H), 5.93 (d, *J* =7.5 Hz, 1H), 4.89–4.95 (m, 1H), 4.71–4.76 (m, 1H), 3.89–4.03 (m, 2H), 1.95–2.12 (m, 2H), 1.67–1.68 (m, 2H). ^{13}C NMR (126 MHZ, d_6–DMSO, ppm): 168.2, 167.7, 160.7, 156.7, 152.2, 151.6, 150.9, 145.6, 145.3, 144.6, 142.9, 141.0, 140.4, 137.2, 136.8, 132.4, 132.2, 132.1, 131.0, 130.0, 129.9, 129.8, 129.8, 129.3, 128.4, 128.2, 128.1, 127.9, 127.8, 126.9, 126.8, 126.3, 126.2, 125.3, 123.1, 122.9, 122.7, 121.9, 121.8, 116.5, 51.7, 46.3, 26.2, 23.6. IR (cm^{-1}): *v* = 3430 (m), 3046 (w), 1577 (w), 1540 (w), 1458 (m), 1383 (w), 1351 (w), 1157 (w), 1039 (m), 842 (s), 742 (s), 695 (w), 676 (w), 557 (m). MS(MALDI-TOF):*m*/*z* 1076.3 (M–PF6). Anal. calcd. For $C_{59}H_{45}F_6IrN_7SP$: C 58.02, H 3.71, N 8.03; found: C 58.52, H 3.85, N 8.35.

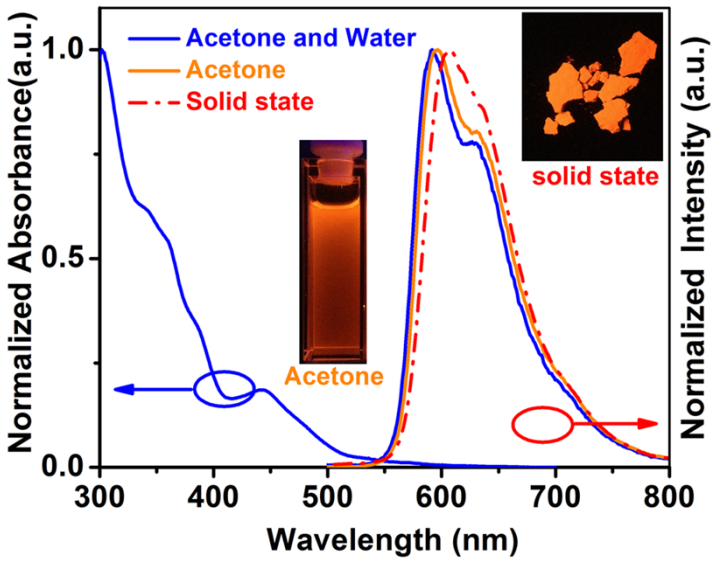

Fig. S3. Normalized absorption spectra and emission spectra of complex **2** in the various states.

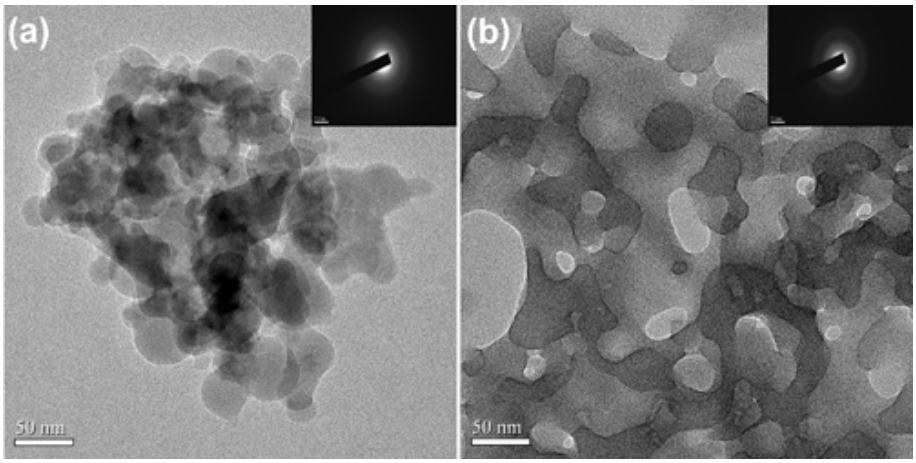

Fig. S4. (a) TEM image of nanoaggregates of complexes **1** and **2** formed in H_2O/CH_3CN mixtures with 90% water fractions. (b) The electron diffraction pattern of the nanoaggregates.

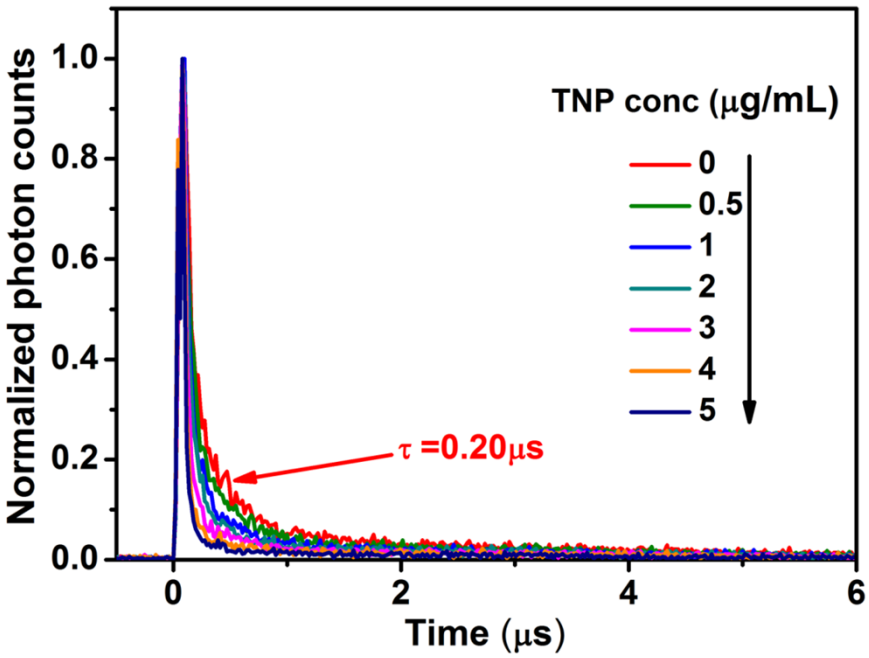

Fig. S5. Lifetime decay profiles of complex **1** in aceton-water (v:v =1:9) mixtures containing different amounts of TNP (from 0 to 5 ppm)

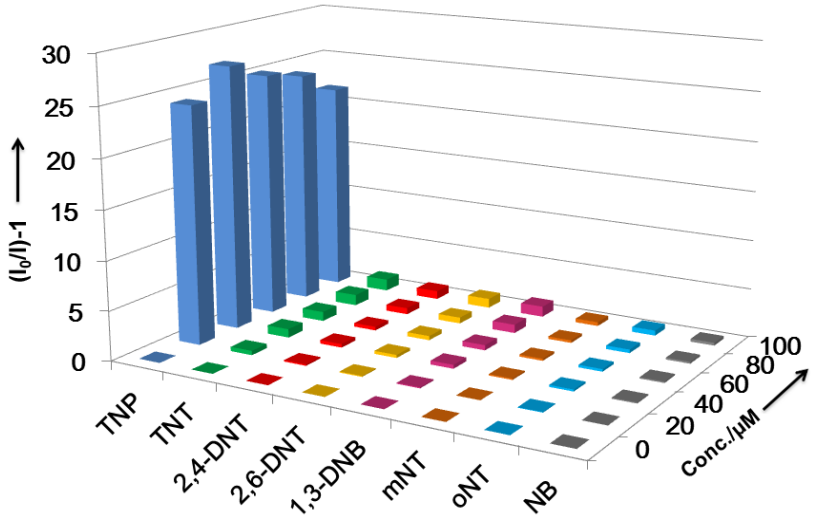

Fig. S6. Quenching efficiency for a given ratio of complex **1** and analytes (1:1 by molar) in aceton-water (v:v =1:9) mixtures.

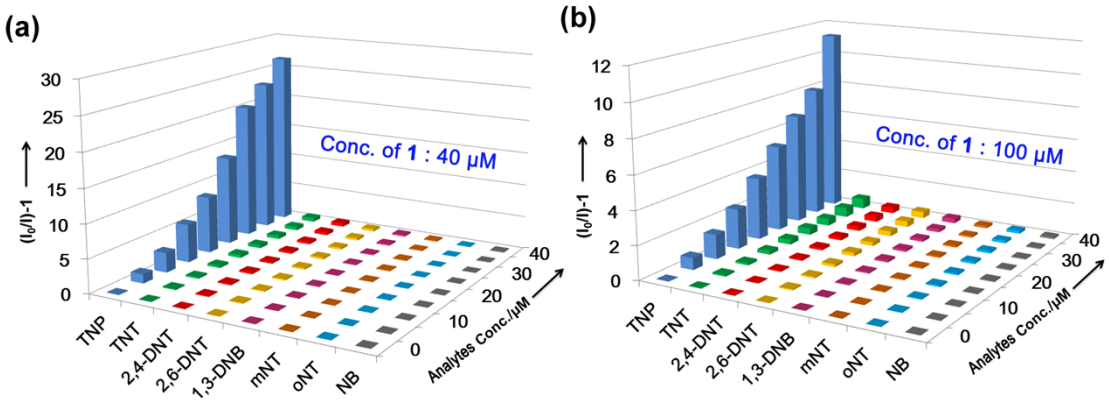

Fig. S7. Stern-Volmer plots of nitro compounds to the emission of complex **1** in aceton-water (v:v =1:9) mixtures.

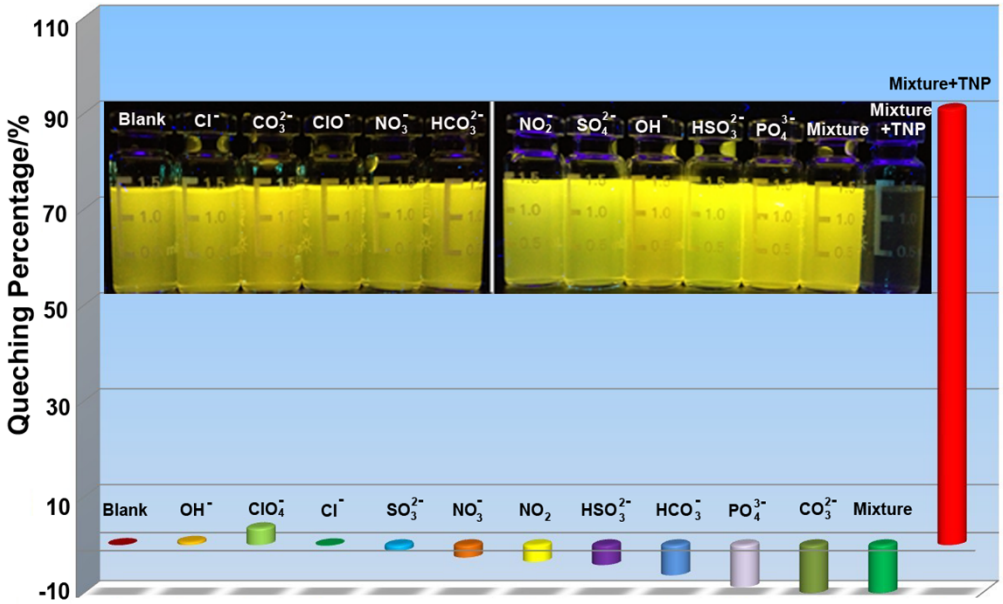

Fig. S8. Percentage of emission quenching of complex **1** in aceton-water (v:v =1:9) system with different anoins of 20 ppm and their mixture with each anoin of 10 ppm followed by TNP. Inset: the luminescence photographs of detected system with various chemical species under a 365 nm UV lamp.

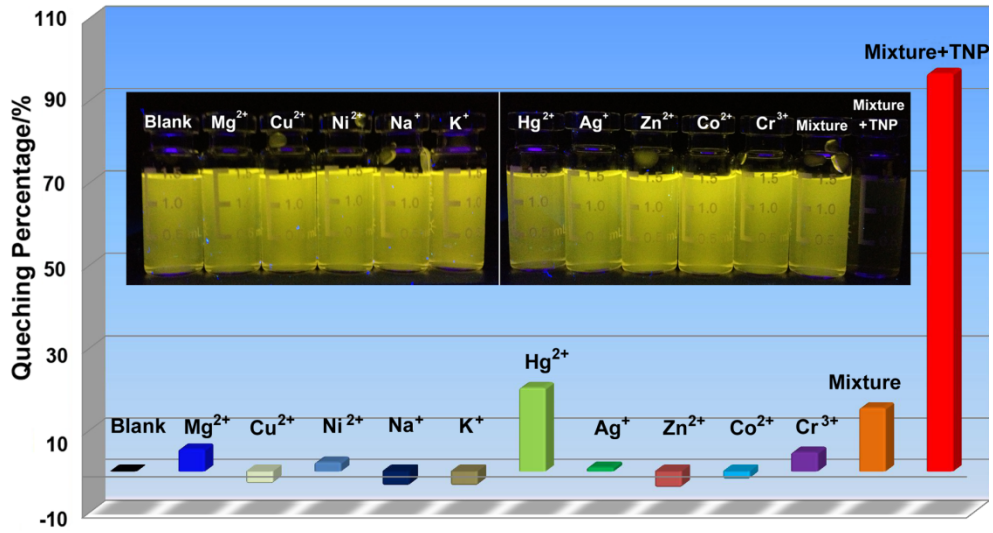

Fig. S9. Percentage of emission quenching of complex **1** in aceton-water (v:v =1:9) system with different cations of 20 ppm and their mixture with each cation of 10 ppm followed by TNP. Inset: the luminescence photographs of detected system with various chemical species under a 365 nm UV lamp.

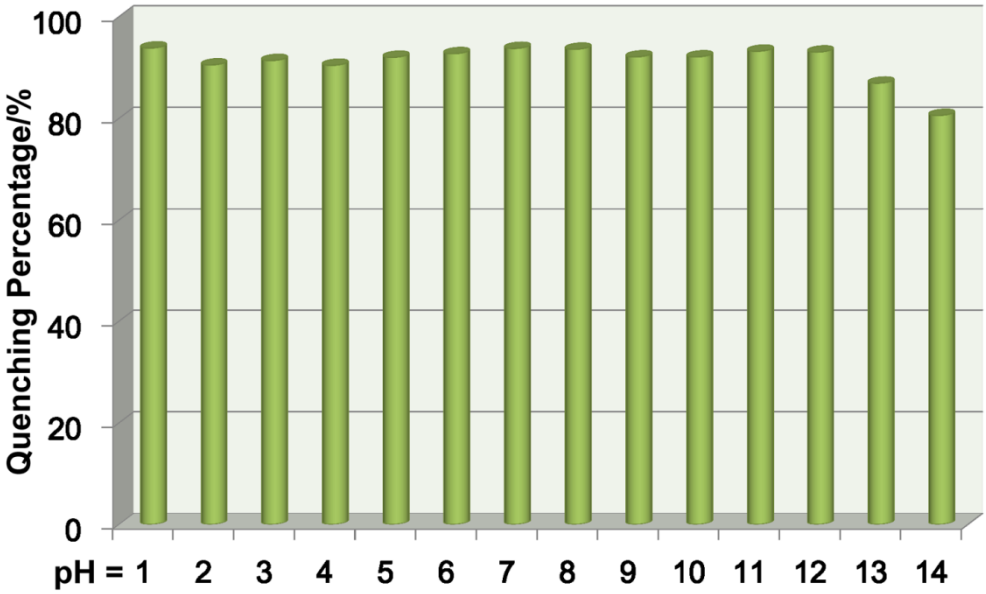

Fig. S10. The effect of pH on Percentage of emission quenching of complex **1** in aceton-water (v:v =1:9) system containing 5 ppm TNP.

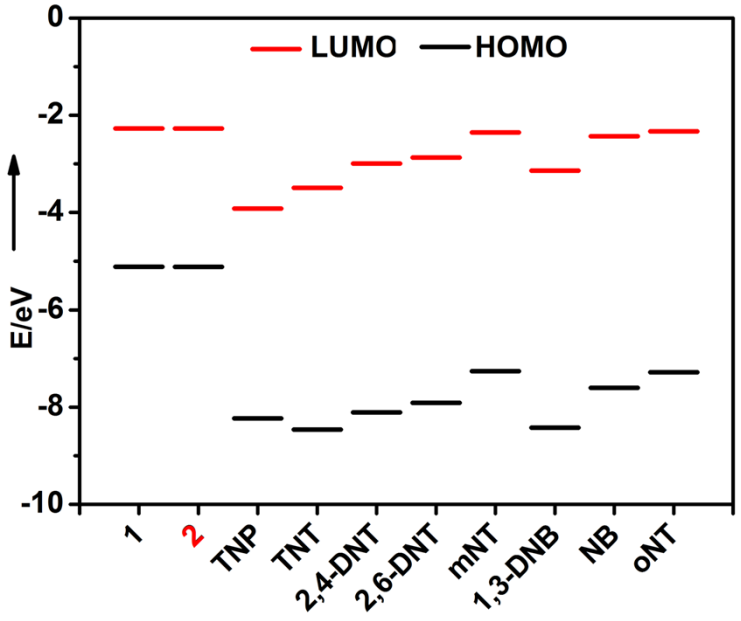

Fig. S11. Calculated HOMO and LUMO energies of complexes **1**, **2** and the analytes.

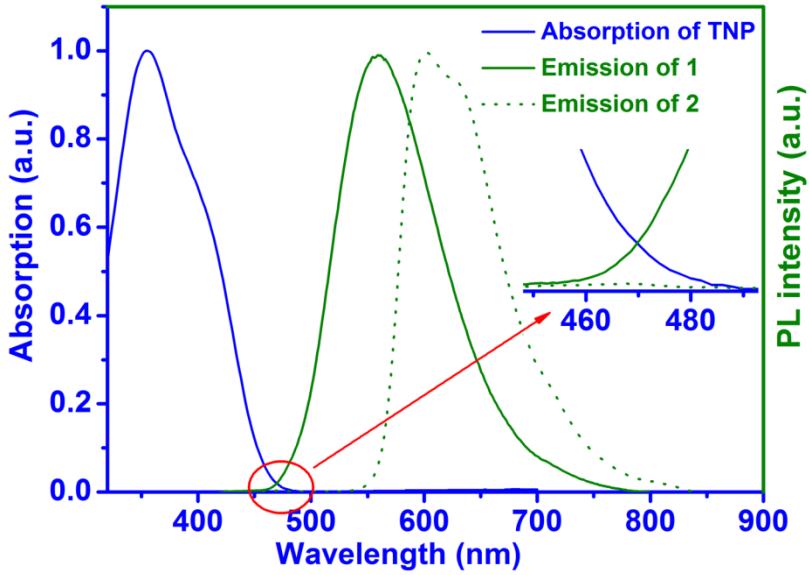

Fig. S12. Absorption spectra of TNP and emission spectra of complexes **1** and **2** in acetone–water (V/V = 1: 9) mixtures. The spectral overlap between the emission of **1** and **2** and the absorption of TNP was shown in inset.

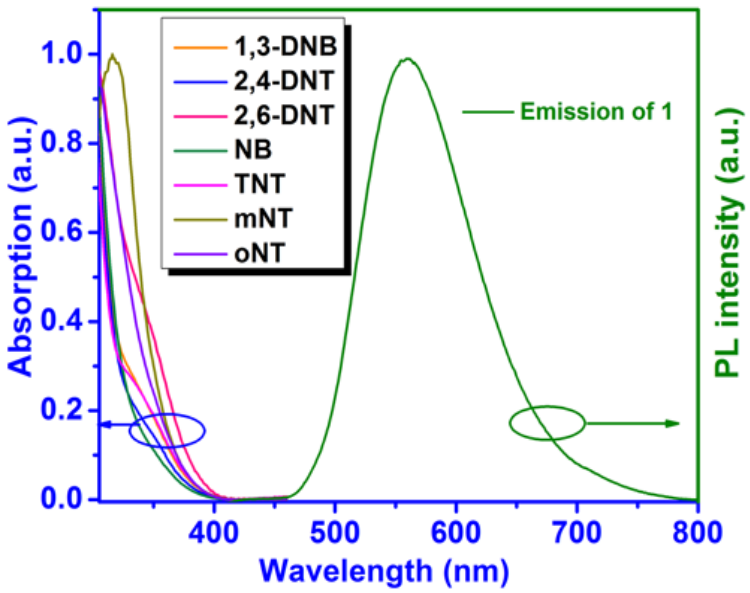

Fig. S13. Absorption spectra of each nitro compounds and emission spectrum of complexes **1** in acetone–water (v/v = 1: 9) mixtures.

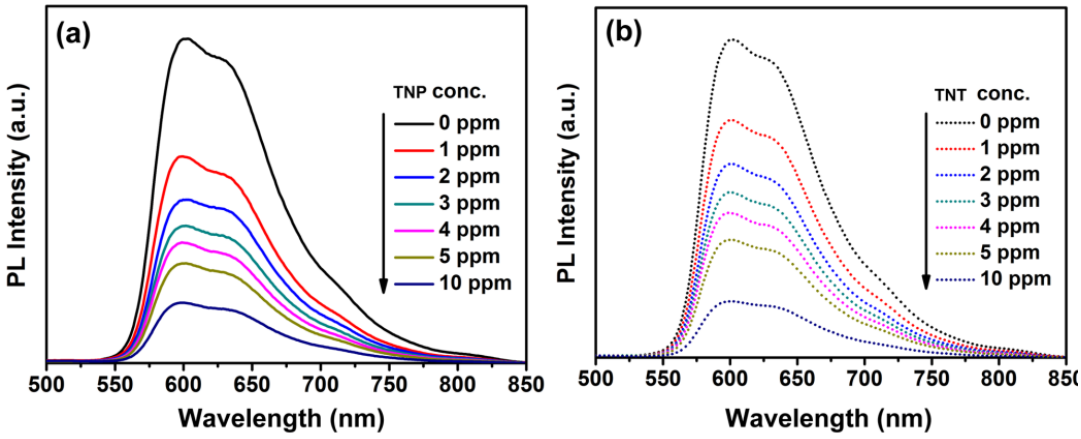

Fig. S14. Photoluminescence spectra of complex **2** in acetone–water (v/v = 1: 9) containing different amounts of TNP (a) and TNT (b).

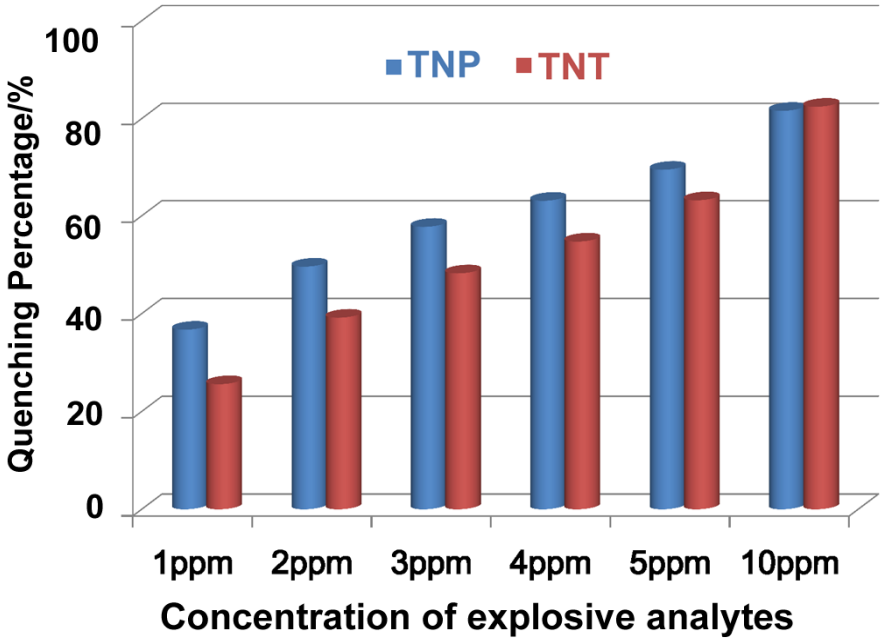

Fig. S15. Quenching percentage obtained for complex **2** in acetone–water (v/v = 1: 9) mixtures toward different concentration of TNP and TNT.

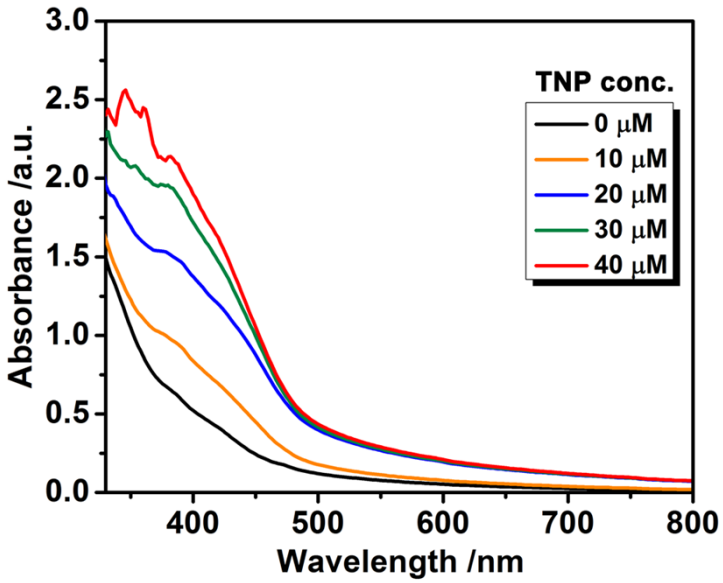

Fig. S16. Absorption spectra of complex **1** with different concentrations of TNP in acetone–water (v/v = 1: 9) mixtures.

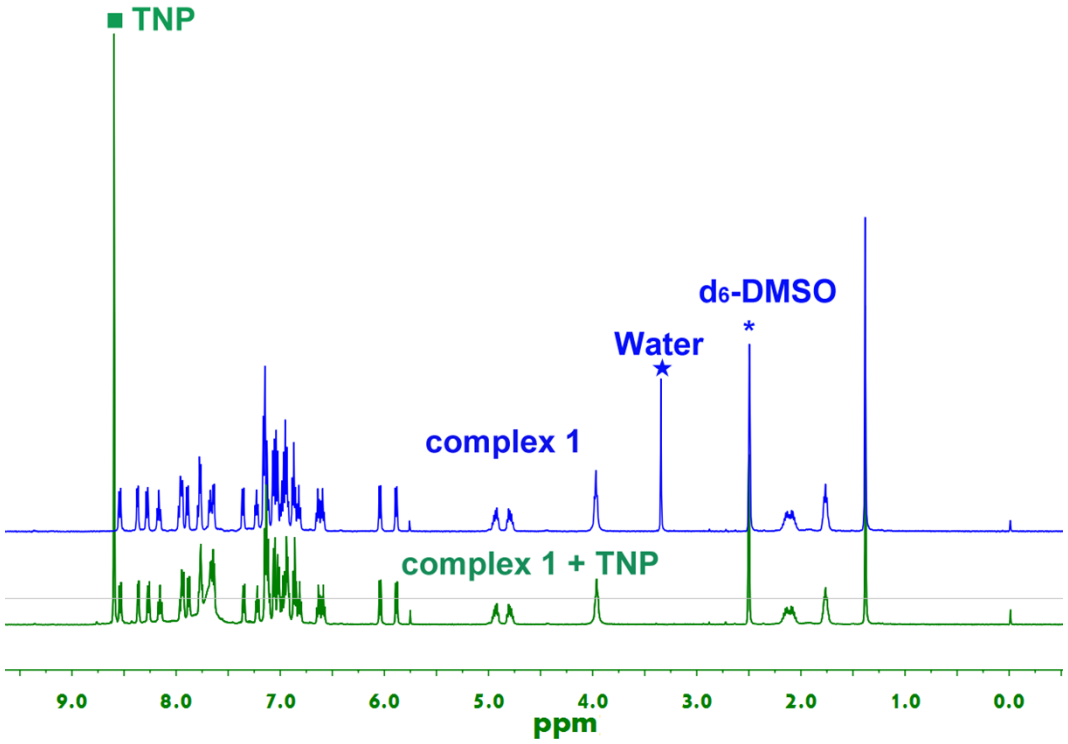

Fig. S17. ^{1}H NMR spectra of complex **1** before and after addition of same quality of TNP.

Fig. S18. Luminescent photographs of TLC plates impregnated by complex **1** against 5 ppm different of nitro compounds.

References

1. M. J. Frisch, G. W. Trucks, H. B. Schlegel, G. E. Scuseria, M. A. Robb, J. R. Cheeseman, G. Scalmani, V. Barone, B. Mennucci, G. A. Petersson, H. Nakatsuji, M. Caricato, X. Li, H. P. Hratchian, A. F. Izmaylov, J. Bloino, G. Zheng, J. L. Sonnenberg, M. Hada, M. Ehara, K. Toyota, R. Fukuda, J. Hasegawa, M. Ishida, T. Nakajima, Y. Honda, O. Kitao, H. Nakai, T. Vreven, J. A. Montgomery, Jr., J. E. Peralta, F. Ogliaro, M. Bearpark, J. J. Heyd, E. Brothers, K. N. Kudin, V. N. Staroverov, R. Kobayashi, J. Normand, K. Raghavachari, A. Rendell, J. C. Burant, S.

S. Iyengar, J. Tomasi, M. Cossi, N. Rega, J. M. Millam, M. Klene, J. E. Knox, J. B. Cross, V. Bakken, C. Adamo, J. Jaramillo, R. Gomperts, R. E. Stratmann, O. Yazyev, A. J. Austin, R. Cammi, C. Pomelli, J. W. Ochterski, R. L. Martin, K. Morokuma, V. G. Zakrzewski, G. A. Voth, P. Salvador, J. J. Dannenberg, S. Dapprich, A. D. Daniels, O. Farkas, J. B. Foresman, J. V. Ortiz, J. Cioslowski and D. J. Fox, Gaussian 09W, Revision A.02; Gaussian, Inc., Wallingford CT, 2009.

2. E. Orselli, G. S. Kottas, A. E. Konradsson, P. Coppo, R. Frohlich, L. De Cola, A. van Dijken, M. Büchel and H. Börner. *Inorg. Chem.,* 2007, **46**, 11082.